ISSN 2717-7203

JOURNAL OF ADVANCES IN MANUFACTURING ENGINEERING

JAME

Volume 4
Number 2
Year 2023 - December

YTÜ PRESS

www.jame.yildiz.edu.tr

ISSN 2717-7203

JOURNAL OF ADVANCES IN MANUFACTURING ENGINEERING

Volume 4 Number 2 Year 2023 - December

ISSN 2717-7203

JOURNAL OF ADVANCES IN MANUFACTURING ENGINEERING

JAME

Volume 4 Number 2 Year 2023 - December

Abstracting and Indexing: Bielefeld Academic Search Engine (BASE), ResearchBible, Directory of Research Journals Indexing (DRJI)

Journal Description: The journal is supported by Yildiz Technical University officially, and is a blind peer-reviewed free open-access journal, published bimontly (June-December).

Publisher: Yildiz Technical University

Editor-in-Chief: Prof. Mihrigul Altan

Language of Publication: English

Frequency: 2 Issues

Publication Type: Online e-version

Publisher: Kare Yayıncılık

ISSN 2717-7203

JOURNAL OF ADVANCES IN MANUFACTURING ENGINEERING

JAME

CONTENTS

J Adv Manuf Eng, Vol. 4, Issue. 2, pp. 35–45, December, 2023

Journal of Advances in Manufacturing Engineering
Web page info: https://jame.yildiz.edu.tr
DOI: 10.14744/ytu.jame.2023.1366597

Original Article

Experimental investigation and optimization of hybrid turning of Ti6Al7Nb alloy under nanofluid based MQL by TOPSIS method

Erkin DUMAN[*1], **Yusuf Furkan YAPAN**[2], **Mehmet Alper SOFUOĞLU**[3]

[1]*Department of Machine and Metal Technology, Gedik Vocational School, İstanbul Gedik University, İstanbul, Türkiye*
[2]*Department of Mechanical Engineering, Yıldız Technical University, İstanbul, Türkiye*
[3]*Department of Mechanical Engineering, Eskişehir Osmangazi University, Eskişehir, Türkiye*

ARTICLE INFO

Article history
Received: 26 September 2023
Revised: 06 November 2023
Accepted: 26 November 2023

Key words:
Ultrasonic vibration assisted machining, minimum quantity lubrication, machining response, titanium alloy, TOPSIS.

ABSTRACT

The present work aims to decide on machining parameters and enhance machinability of the biomedical Ti6Al7Nb alloy using nanofluid MQL with nanoparticles of graphene (NMQL) and ultrasonic vibration assisted (UVA) machining methods were applied both separately and in a hybrid manner. Consequently, for the chosen cutting parameters, when compared to the conventional turning (CT) with vegetable cutting oil-based MQL, the UVA-NMQL hybrid method has achieved a reduction in cutting forces ranging from approximately 11% to 23%, a decrease in cutting temperatures by around 9% to 17%, and an enhancement in average surface roughness by roughly 15% to 53% across all the analyzed results compare to vegetable oil based conventional MQL turning conditions. Additionally, using the Technique for Order of Preference by Similarity to Ideal Solution (TOPSIS) method, the optimum cutting parameters were determined as UVA-NMQL cutting condition, 130 m/min cutting speed, and 0.1 mm feed value.

Cite this article as: Duman, E., Yapan, Y. F., & Sofuoğlu, M. A. (2023). Experimental investigation and optimization of hybrid turning of Ti6Al7Nb alloy under nanofluid based MQL by TOPSIS method. *J Adv Manuf Eng*, 4(2), 35–45.

INTRODUCTION

Titanium alloys find extensive utilization in the field of biomedical devices due to their favorable characteristics, including low density, outstanding biocompatibility, exceptional resistance to corrosion, and impressive mechanical properties [1–3]. This is especially notable in load-bearing applications like orthopedic implants [3, 4]. Among titanium alloys, Ti-6Al-7Nb has been successfully used in a range of clinical applications, including hip and knee implants, dental implants, and spinal implants and researchers have reported positive clinical outcomes with this alloy, including reduced complications and improved patient comfort [5–8]. Numerous studies have demonstrated that the alloy is well-tolerated by the human body and exhibits well osteoblast response when implanted [9, 10]. The elasticity modulus of Ti-6Al-7Nb is lower than that of Ti-6Al-4V [11, 12]. As a result of this, Ti-6Al-7Nb alloy facilitates better integration with bone and potentially leads to less stress shielding in load-bearing areas [13]. Moreover, Ti-6Al-4V alloy comprisal vanadium, which possesses toxic properties, limits the use of this alloy in biomedical applications [14, 15]. Therefore, the Ti-6Al-7Nb alloy stands apart from other titanium alloys in biomedical applications. On the contrary, Ti-6Al-7Nb alloy are often categorized as difficult-to-cut material, primarily due to their inherent properties like high strength and hardness, low thermal conductivity etc. [16]. These properties lead to rapid tool wear and plastic deformation of cutting tools reported by researchers [17, 18]. For instance, Risco-Alfonso et al. [19] conducted turning exper-

***Corresponding author.**
*E-mail address: erkinnduman@gmail.com

Table 1. Experimental plan

Experiment no	Cooling type	Cutting speed (m/min)	Feed rate (mm/rev)
1	MQL	70	0.1
2	MQL	70	0.14
3	MQL	100	0.1
4	MQL	100	0.14
5	MQL	130	0.1
6	MQL	130	0.14
7	UVA-MQL	70	0.1
8	UVA-MQL	70	0.14
9	UVA-MQL	100	0.1
10	UVA-MQL	100	0.14
11	UVA-MQL	130	0.1
12	UVA-MQL	130	0.14
13	NMQL	70	0.1
14	NMQL	70	0.14
15	NMQL	100	0.1
16	NMQL	100	0.14
17	NMQL	130	0.1
18	NMQL	130	0.14
19	UVA-NMQL	70	0.1
20	UVA-NMQL	70	0.14
21	UVA-NMQL	100	0.1
22	UVA-NMQL	100	0.14
23	UVA-NMQL	130	0.1
24	UVA-NMQL	130	0.14

MQL: Minimum quantity lubrication; UVA-MQL: Ultrasonic vibration assisted-MQL; NMQL: Nanofluid MQL that is containing 0.8% graphene by weight; UVA-NMQL: Ultrasonic vibration assisted – nanofluid added MQL

iments on Ti-6Al-7Nb alloy using ceramic tools under dry cutting conditions. Their results showed that at the cutting speed of 200 m/min, the tool life was limited to only 6 minutes. While such tool life may be acceptable for many steel materials, it is notably high for machining this particular alloy. Carvalho et al. [17] focused on the dry turning of the Ti-6Al-7Nb alloy. In all the chosen cutting conditions, the chips did not break, and instead, they obtained unsuitable segmented and long helical ribbon chips. As a consequence of this research, several strategies such as micro cutting, and different cooling and lubrication techniques have been proposed to improve the machinability of Ti-6Al-7Nb alloys including minimum quantity lubrication (MQL) [20], cryogenic and flood coolants [13], micro cutting [21]. Among these strategies, MQL has arisen as a favorable substitute for conventional flood cooling owing to an environmentally conscious method that involves the application of a very small amount of mineral or vegetable oil in mist form, delivered by a compressed air stream (typically 5–7 bar), directly to the cutting zone [22]. MQL has demonstrated remarkable performance in turning, milling, and grinding operations by penetrating the cutting zone and providing essential lubrication [23]. The implementation of this method has greatly aided in enhancing the chip forming process of numerous engineering alloys. For instance, in steel machining, Jagatheesan et al. [24] revealed that comparison to traditional dry cutting and flood machining, the MQL method has achieved a reduction of approximately 20% in cutting forces and 12% in cutting temperature, thereby yielding an improved surface quality. Similarly, Kannan et al. [25] demonstrated the impact of the MQL method on reducing tool wear and cutting forces in the machining of aluminum alloy and its composites. Furthermore, Gong et al. [26] conducted a study on the impact of the MQL method on surface integrity during the machining of Inconel 718 alloy. The MQL method diminished surface defects, and creates a smoother surface compared to dry and flood cutting, with fewer marks and adhered particles to it.

Nowadays, there has been a growing adoption of nanoparticle-added super lubricants to improve the effectiveness of MQL in machining [27, 28].

Multiple types of nanoparticles, such as Al_2O_3 [29], MoS_2 [30], CuO [31], zinc oxide (ZnO) [32], carbon nanotube [33], and graphene [26] etc. have been employed for the purpose of nanofluid preparation and subsequent examination of their effects. Therefore, super lubricity has garnered significant global interest at a time when humanity is facing a critical energy crisis [34]. Among these, graphene is one

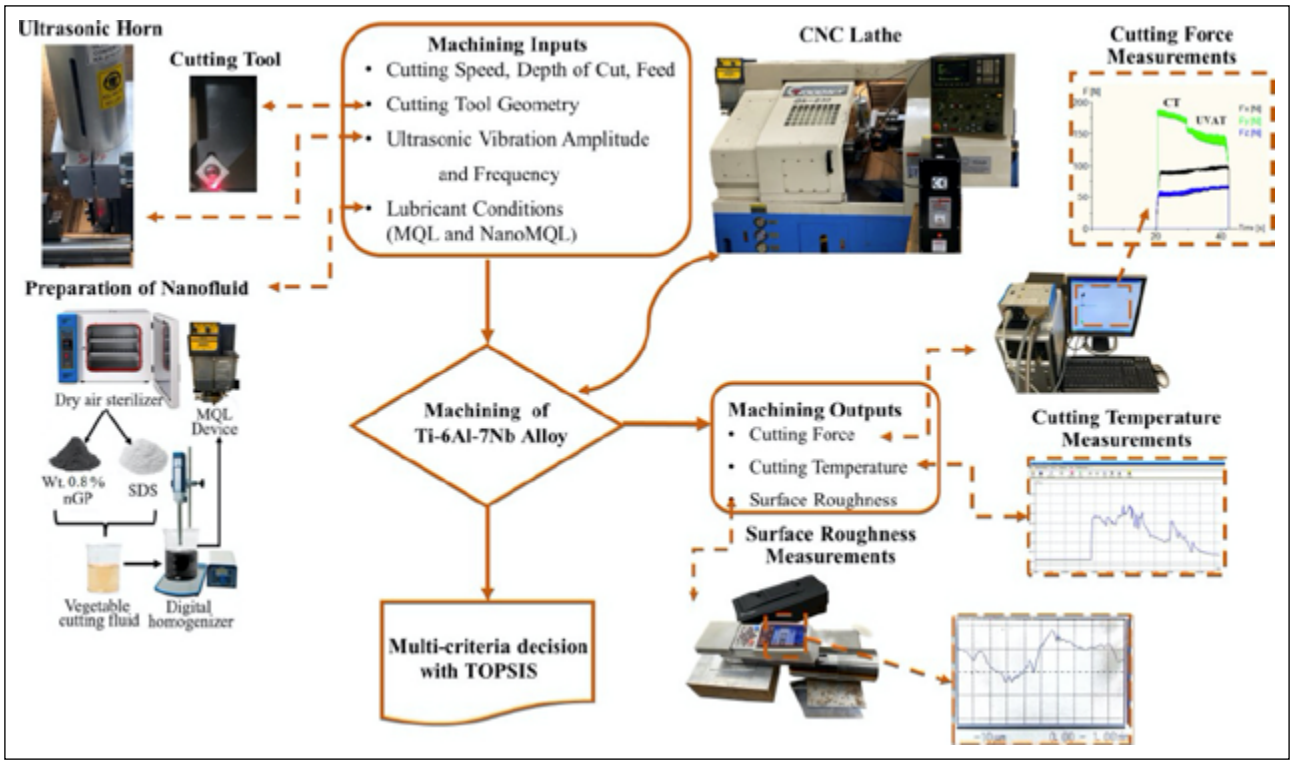

Figure 1. Flow chart of experimental methodology.

of the super lubricants and it is an extremely thin material at the atomic level, possessing a low surface energy that has the potential to reduce both friction and adhesion [35]. As a result, it has been increasingly employed in machining applications as both a coolant and a lubricant.

Lately, nontraditional machining methods have been employed in addition to conventional cooling and lubrication conditions to enhance the machinability of difficult to cut materials. One of these methods is ultrasonic vibration assisted (UVA) machining. Vibration-assisted machining involves the application of vibrations to either the cutting tool or the workpiece, typically at specific frequencies and amplitudes. This method offers distinct advantages, particularly when dealing with difficult-to-machine materials, in comparison to conventional machining approaches. It effectively mitigates undesirable noise, reduces tool wear, and enhances the surface finish of the machined workpiece [36]. Koshimizu et al. [37] investigated ultrasonic vibration machining of Ti-6Al-4V alloy. They found that applying ultrasonic vibration to the tool tip reduced cutting force and improved tool wear and surface roughness [37]. Kandi et al. [38] investigated ultrasonic vibration-assisted turning and discovered reductions in cutting forces and surface roughness for Ti-6Al-4V alloy. Furthermore, studies have shown that combining MQL and ultrasonic-assisted machining improves the performance of difficult-to-cut materials. For instance, Airao et al. [39] investigated the use of hybrid conditions involving MQL, cryogenic cooling and lubrication in the ultrasonic turning of Inconel 718 alloy. The results demonstrated that this hybrid machining approach significantly reduced flank wear by 32–53%, power consumption by 11–40%, and power consumption by 5–31% [9].

In light of the studies mentioned in the literature review, the need to try new strategies to improve the machining of Ti-6Al-7Nb alloy exists. The main objective of this work is to investigate the machinability of the Ti-6Al-7Nb alloy using the MQL (Minimum Quantity Lubrication) method and to gain a better understanding of the impact of applying ultrasonic vibration and MQL with the addition of nanographene (NMQL) to the cutting tool on machining performance. In the second phase of this study, in order to determine the optimum cutting parameters for machining this alloy using the selected methods, the Technique for Order of Preference by Similarity to Ideal Solution (TOPSIS) method was employed to determine the optimum cutting parameters.

MATERIALS AND METHODS

In this work, biomedical grade Ti-6Al-7Nb alloy work material was used in order to perform machining experiments. The work material has 883 MPa yield strength, and 946 MPa ultimate tensile strength. Initial diameter of 60 mm and a length of 130 mm as indicated in Figure 1. GOODWAY GA-230 CNC lathe with a main power of 11 kW and a spindle speed up to 4200 rpm was utilized to carry out oblique cutting experiments. The machining length and depth of cut were kept constant at 15 mm and 1 mm respectively. The cutting tool insert utilized was of the uncoated tungsten carbide type Sandvik SCMT 120408-KM H13A with SSSCL 2525 M12 tool holder. The plan used in machining experiments is given in Table 1.

In ultrasonic tests, an ultrasonic horn, ultrasonic generator and power unit were employed with supply voltage

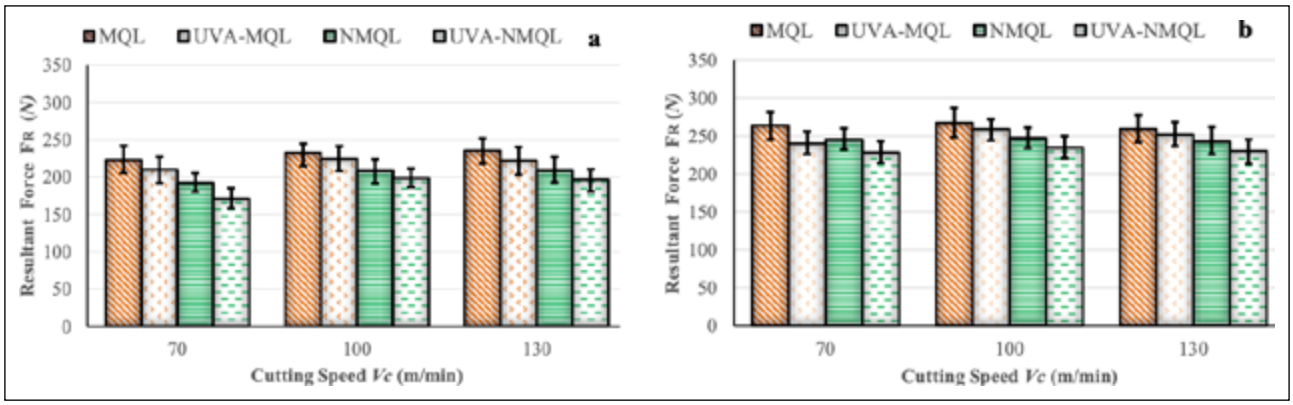

Figure 2. Variation of resultant cutting force vs. cutting conditions at different feed **(a)** 0.1 mm/rev and **(b)** 0.14 mm/rev.

with 230 V/50-60 Hz, and the frequency of the vibration was about 20 kHz detected by the oscilloscope-indicator, while the amplitude was measured 20 µm. Additionally, vibration was given to the cutting tool in a direction that was transverse to the main cutting force axis. An MQL device is employed for delivering commercial vegetable cutting fluid to the cutting zone. It operated with a flow rate of 30 mL per hour and maintained a pressure of 5 bar. The MQL nozzle had a diameter of 1 mm, and it was positioned at an angle of 30°. At stage of the nanofluid, nano graphene particles were used with a particle size of 4–8 µm, gray-colored, had a purity of 99%, a surface area of 110–130 m^2/g, a thickness of 5–10 nm, and a density of 2 g/cm^3. The particles were spread into a glass container and subjected to a 75-minute moisture removal and drying process in an oven at a temperature of 120 °C. The dried nano particles were weighed on a precision balance and mixed with vegetable cutting oil at a ratio of 0.8% by weight. To enhance the homogeneity of the nGP nanofluid and limit clumping and sedimentation times, SDS (Sodium Dodecyl Sulfate) was added at a ratio of 0.1% by weight of graphene. Finally, the prepared mixtures were stirred for 60 minutes at 5000 rpm using a digital homogenizer. The procedure for preparing the nanofluids is shown in Figure 1. From the outputs in this study, cutting forces and cutting temperature were measured using the Kistler 9257BA model dynamometer and the Optris – CT laser 3MH1 model double laser contactless temperature measurement respectively. Besides, A Mitutoyo SJ-210 surface roughness tester was used to measure machined surface roughness values. The flow chart of experimental methodology is depicted in Figure 1.

RESULTS AND DISCUSSION

Analysis of Resultant Force

The cutting force is considered a vital aspect of the chip removal process. Various factors impact these cutting forces, such as cutting speed, feed, depth of cut, cutting tool, and the type of cutting fluid in use. Resultant force is calculated by utilizing Eq.1 [40]

$$F_R^2 = F^2x + F^2y + F^2z \quad (1)$$

Here, FR is the resultant force, Fx, Fy and Fz represent radial cutting force, main cutting force, and feed force respectively [40]. Calculated resultant force results are depicted at the feed rate of 0.1 mm/rev in Figure 2a and 0.14 mm/rev in Figure 2b. The obtained findings have demonstrated that the combination of NMQL (nanographene-added MQL) with ultrasonic vibration-assisted machining has enabled a significant reduction in cutting forces for all selected cutting conditions. For instance, at a cutting speed of 70 m/min and the feed rate of 0.1 mm/rev, the resultant force recorded in the MQL was 223 N, whereas, with the application of UVA-NMQL, the force was measured to be approximately 24% lower at 170 N. When compared to MQL machining, the utilization of UVA-NMQL resulted in about 12% reduction in the resultant force at the cutting speed of 130 m/min and the feed of 0.14 mm/rev. Compared to cutting speed, feed rate has a more significant impact on forces. An increase in feed rate has been observed to lead to an increasing trend in cutting forces for all cutting conditions. For low cutting speed (at 70 m/min) in continuous turning, when feed increased from 0.1 mm/rev to 0.14 mm/rev, the resultant force increased from 225 N to 264 N in MQL and 192 N to 245 N in NMQL. Apparently, the NMQL method has led to lower cutting forces compared to the MQL method. The main reason for this phenomenon is attributed to tremendous properties of nanographene like atomic-level thinness and remarkably low surface energy, offering the promise of decreasing both friction and adhesion [35]. The cutting temperature results shown in Figure 3 qualitatively supports these findings. However, in ultrasonic vibration assisted machining, recorded forces are 210 N to 240 N in UVA-MQL and 171 N up to 228 N in UVA-NMQL for selected feed 0.1 mm/rev and 0.14 mm/rev, respectively. This outcome is probably an effect of the intermittent cutting process introduced through ultrasonic vibration-assisted machining. In conventional continuous turning (CT), the tool maintains constant contact with the workpiece, resulting in relatively elevated resultant forces. Conversely, intermittent cutting features diminish the friction between the tool and workpiece, thereby leading to a reduction in cutting forces observed in ultrasonic vibration assisted turning (UVAT). It's worth noting that when the UVAM and both MQL and NMQL methods are used simultaneously, the lubrication and cooling performance of MQL can be further improved. This phenomenon has

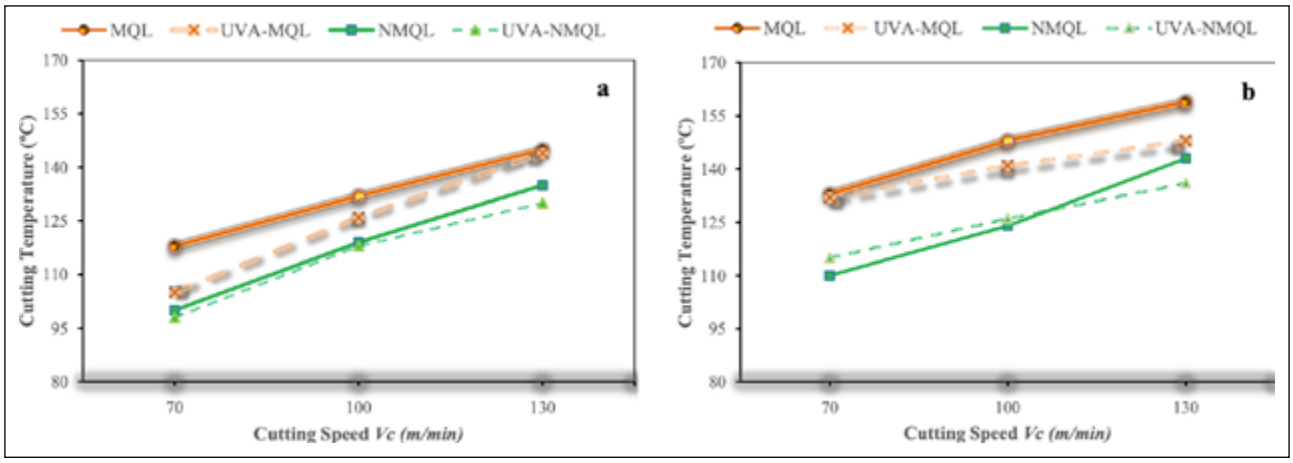

Figure 3. Cutting temperature variation for different cutting conditions and feed **(a)** 0.1 mm/rev; **(b)** 0.14 mm/rev.

been explained due to the separate-type cutting mechanism of UVAM and cavitation phenomenon of the resonant workpiece [41]. It has been reported that using UVA and MQL simultaneously has a coupling effect [42]. When high temperature thermal stress and poor friction qualities cause microcracks and friction traces to emerge on the tool surface, UVAMQL can effectively alleviate these problems reported by Ni et al. [43].

Cutting Temperature

Low thermal conductivity (6.6–6.8 W/m.K) of titanium alloys leads to elevated heat generation during the machining of these alloys due to the plastic deformation and friction effects at the tool-chip interface and shear plane [40, 44, 45]. Therefore, cutting temperature is a critical factor for understanding the machining performance of titanium alloys. Figure 3 displays cutting temperature variation for different cutting conditions.

In this study, it was observed that the implementation of MQL resulted in the attainment of the highest recorded temperature of 159 °C. This temperature was achieved under the cutting conditions of a speed of 130 m/min and a feed rate of 0.14 mm/rev. However, thanks to the employment of NMQL the cutting temperature decreased by approximately 10%, measuring 143 °C. However, at a relatively lower cutting speed of 70 m/min, a more significant reduction of approximately 17% in temperature was achieved with NMQL. These findings can be attributed to its high thermal conductivity and lubrication properties resulting from the presence of graphene. Moreover, compressed air improves cooling and nanofluid lubricates machining interfaces by providing rolling effect and protective film [30]. The friction coefficient, thermal conductivity, and dynamic viscosity of cutting oil are also critical parameters for heat transfer. These parameters are predominantly influenced by the tribological and thermophysical characteristics of the prepared nanofluid. However, formation of a tribofilm in cutting zone is attributed not only to lubrication but also to the application of air at a specific pressure in the MQL method. Obikawa et al. [46] tested the effectiveness of the MQL system at air pressure values ranging from 3 to 7 bar. They found that an increase in air pressure reduced tool wear. On the other hand, Li and Liang [47] focused on convective heat transfer separately for air and oil in the MQL method. In a study conducted by Kurgin et al. [48], the effect of different air pressure and oil flow rates on the convective heat transfer coefficient in the MQL technique was investigated. Another study by Gong et al. [26] found that the specific heat capacities of cutting oil and graphene nanoparticles suspended in NMQL techniques varied. Added graphene nanoparticle increased the MQL-specific heat capacity by 11%. Based on the literature review, the MQL method used in this study was conducted with a vegetable-based cutting oil with a thermal conductivity of 0.5–1 W/m.K [18]. In contrast, graphene is produced from synthetic graphite powder [19] and graphene nanoparticles can exhibit an impressive thermal conductivity of up to 3000–5500 W/m.K [20, 21]. Consequently, graphene added nanofluid based MQL (NMQL) is improve heat transfer. At a high cutting speed of 130 m/min and feed of 0.14 mm/rev, the effectiveness of NMQL was found to diminish. This can be attributed to insufficient time for cooling and diffusion processes. On the other hand, the lowest cutting temperature was achieved under the UVA-NMQL condition. The application of the NMQL method in conjunction with ultrasonic vibration significantly reduced the cutting temperature. As a result of the intermittent cutting process between the tool-workpiece pair in ultrasonic vibration-assisted machining, long-term extrusion between the workpiece and tool free surface, as well as chip removal on the tool free surface, is interrupted. This situation leads to a reduction in plastic deformation in the chip deformation zone, resulting in a decrease in cutting temperature [16]. It is understood that the ultrasonic vibration-assisted machining process provides a significant decrease in cutting temperature as a result of the intermittent cutting process and the separation of the tool-workpiece pair.

Surface Roughness

Essential surface roughness values within nominal limits are expected in biomedical applications in order to ensure conformity between tissue and implants [49–51].

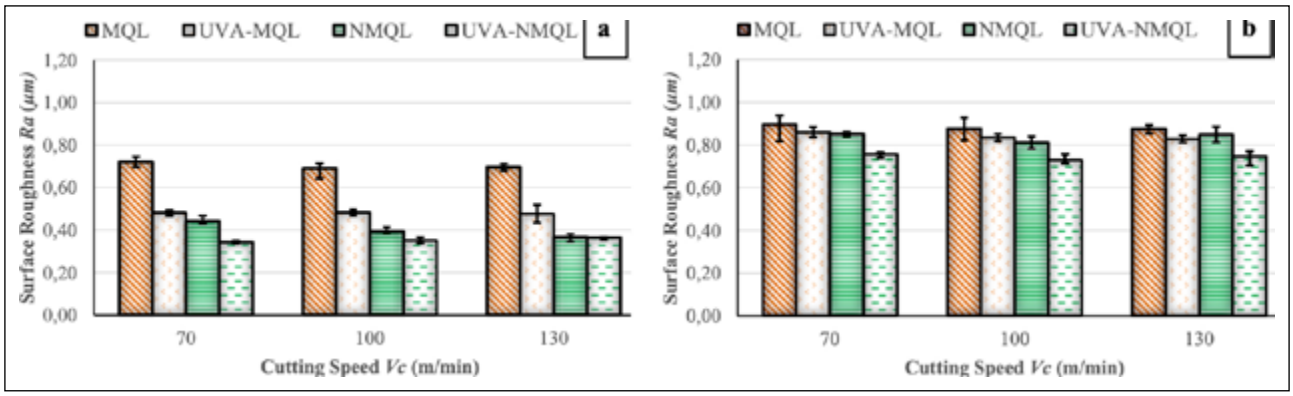

Figure 4. Surface roughness variation for different cutting conditions and feed **(a)** 0.1 mm/rev; **(b)** 0.14 mm/rev.

Moreover, machining process generates smoother surfaces and thereby corrosion resistance, fatigue life etc. characteristics have been influenced at the end of the process [52]. Therefore, average surface roughness values of processed samples subjected to CT and UVA machining under variable cutting parameters and conditions have been examined. The measured surface roughness results are presented in Figure 4.

It can be seen that the surface roughness values obtained are below 1 µm under all cutting speeds and cutting conditions. A higher roughness peak was measured in MQL machining at the feed of 0.1 mm/rev, whereas the lowest roughness values have been obtained with nano graphene particle added MQL and ultrasonic vibration-assisted machining (UVA-NMQL).

In comparison with MQL, it was evident that decreasing of surface roughness by approximately 30%, 44% and 49% under UVA-MQL, NMQL and UVA-NMQL, respectively when the cutting speed was 100 m/min and the feed rate was 0.1 mm/rev. The ability of graphene nanoparticles to reduce the coefficient of friction is the reason for this phenomenon [53]. Moreover, in MQL machining, at the cutting speed of 130 m/min and feed rate of 0.1 mm/rev, the application of ultrasonic vibration to the cutting tool (UVA-MQL) reduced the surface roughness by 32%. Ni et al. [43] conducted experiments using CT, MQL, and MQLUVAM methods separately in the milling process of the Ti-6Al-4V alloy. They reported that the simultaneous application of the UVAM and MQL methods resulted in a synergistic effect, which considerably reduced cutter tool wear and minimized the formation of microcracks in the tool. As a result, the surface quality of the UVAMQL method was significantly improved [43]. It is reasonable to expect that using the UVAM and MQL methods simultaneously will produce excellent microtextured surfaces. However, when a feed rate of 0.14 mm/rev was chosen, this positive effect dramatically decreased, and the impact of ultrasonic vibration on reducing surface roughness was approximately 6%. On the other hand, all measured surface roughness values are smaller than the predicted average roughness value according to Equation (2) [40], which were calculated as 0.39 µm, and 0.77 µm for 0.1 mm/rev and 0.14 mm/rev feed, respectively.

$$Ra = \frac{f^2}{32 r_c} \tag{2}$$

where f is the feed and r_c is the depicted corner radius of the tool.

Multi-Criteria Decision Making with TOPSIS

In the realm of manufacturing and machining, achieving optimal performance in machining processes is paramount for ensuring product quality, energy efficiency, and cost-effectiveness [54]. The quest for excellence in machining operations necessitates a meticulous analysis of process parameters to attain the finest balance between multiple conflicting objectives such as minimizing cutting force and cutting temperature, maximizing material removal rates, and ensuring surface finish quality. To address these multifaceted concerns, researchers and engineers have turned to Multi-Criteria Decision-Making (MCDM) methods as a powerful approach for optimizing the machining process [55]. Among the various MCDM techniques, the Technique for Order of Preference by Similarity to Ideal Solution (TOPSIS) method stands out as a robust and versatile tool that can be adeptly applied to the domain of machining optimization.

Prior to assessing the proximity of the outcomes to the ideal outcome in the TOPSIS methodology, it is necessary to compute the weighted efficiency distributions of the respective activities. The distribution of efficacy can be assigned uniformly across all outcomes or determined by the researcher through their expertise or mathematical equations. In this study, the equations presented by Saatçi et al. [56] were used to calculate the efficiency distributions. The method used to calculate the weighted efficiency distributions here is the entropy method. The distributions of the results' weighted efficiencies were determined as 0.228, 0.268, 0.234, and 0.27 for cutting force, surface roughness, cutting temperature, and material removal rate, respectively. Following the computation of the outcomes' weighted efficiency distributions, the TOPSIS decision-making method operates. In the presented study, while the material removal rate was maximized, the cutting force, cutting temperature, and surface roughness were minimized and sorted according to the closeness to the ideal solution. The TOPSIS method proposed by Ous-

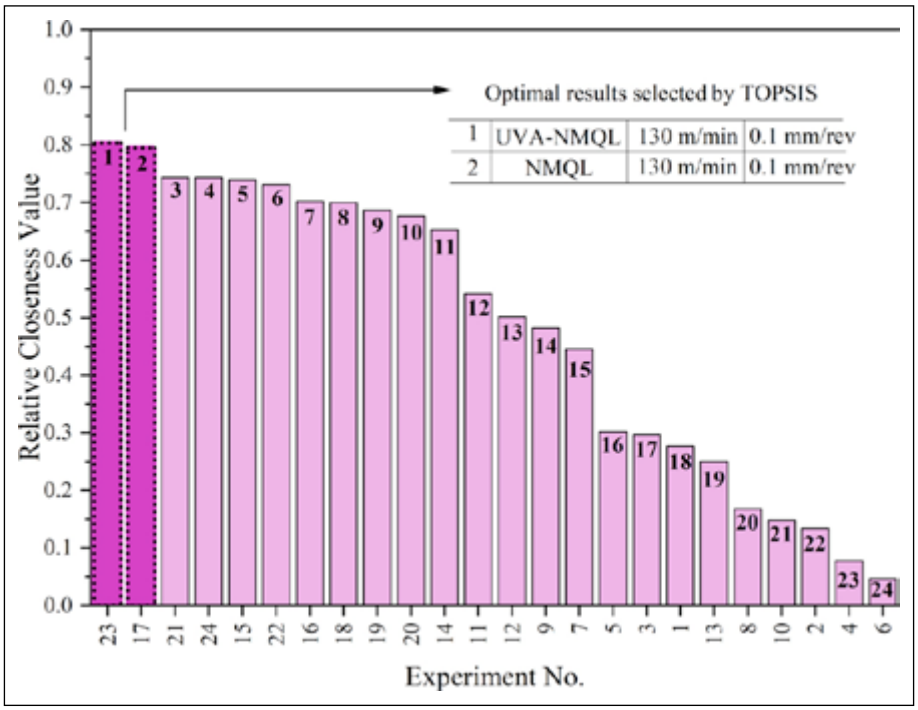

Figure 5. Optimal results selected by the TOPSIS.

sama et al. [57] and applied in this study includes the stages of normalization of the decision matrix, calculation of the weighted normalized decision matrix, calculation of the negative and positive values of the ideal solutions, calculation of the distance between each alternative solution and the positive and negative ideal solution, and ranking the solutions in descending order. Consequently, the optimal results obtained through the TOPSIS method are presented in Figure 5. The best result, which reduces cutting force and cutting temperature and increases material removal rate and surface quality, was obtained at the cutting speed of 130 m/min and at the feed rate of 0.1 mm/rev under UVA-NMQL cutting conditions. This was followed by using a cutting speed of 130 m/min and the feed rate value of 0.1 mm/rev under the NMQL cutting condition. It is clear from the TOPSIS decision-making process that a low feed value is the best option. A similar result was presented by Saatçi et al. [56] in the orthogonal turning of AISI 310S stainless steel to obtain minimum cutting force, machining cost, and carbon emission in the selection of machining parameters with the TOPSIS method. Additionally, as can be seen from Figure 5, it can be seen that high cutting speed is the best option when evaluated together with the weighted efficiencies obtained in terms of cutting force, cutting temperature, metal removal rate, and surface roughness. Actually, reducing the cutting speed causes a decrease in cutting tool wear, resulting in a decrease in machining costs and carbon emissions resulting from the use of cutting tools [58]. For example, Jawaid et al. [59] determined that the extent of flank wear and cutting edge deformation of the cutting tool increased as the cutting speed increased in the turning of Ti-6246 titanium alloy. However, in terms of sustainable turning, decreasing the cutting speed increases the machining time, thus increasing the energy consumed, resulting in an increase in the total machining cost and carbon emissions [60]. As a result, increasing the cutting speed, reducing the feed rate, and using ultrasonic vibration-assisted machining offers the best results in terms of machining response and sustainability.

CONCLUSIONS

In order to enhance the efficiency of the MQL method employed to achieve sustainable manufacturing objectives, this study investigates the machining performance of the Ti-6Al-7Nb biomedical titanium alloy. It does so by utilizing nano-fluids prepared with the addition of graphene nanoparticles to MQL oil, alongside energy-efficient and power-specific ultrasonic vibration-assisted machining techniques. The analysis focuses on output parameters such as cutting force, cutting temperature, material removal rate and surface roughness. The specific findings obtained from this investigation are outlined below:

1) In experiments conducted using the conventional turning (CT) method, the NMQL method containing 0.8% by weight of graphene has reduced resultant forces by a range of 6% to 14% compared to vegetable-based cutting oil assisted MQL.
2) UVA-NMQL hybrid method has resulted in a reduction in cutting forces by approximately 9% to 19% compared to the UVA-MQL method. Besides, when compared to the traditional MQL method, which generated a resultant force value of 223 N, the UVA-NMQL method reduced the cutting force by approximately 23%, bringing it down to 171 N, which is considered significant for the machining of this alloy.

3) UVA-NMQL method exhibits the lowest cutting temperature. In this study, under high cutting conditions, which are considered to be Vc=130 m/min and f=0.14 mm/rev, the UVA-NMQL method has successfully reduced the cutting temperature by approximately 15%, bringing it down from 159 °C to 136 °C.
4) The hybrid method uses intermittent cutting and the nanofluid containing graphene, which falls into the superlubricant category, in the UVA-NMQL method, resulted in low cutting forces and temperatures, contributing positively to surface roughness. As an example, in the case of the MQL method at the cutting speed of 130 m/min. and the feed rate of 0.1 mm/rev., the average surface roughness, which was initially 0.7 µm, was reduced by approximately 47% to a measurement of 0.37 µm when the UVA-NMQL method was implemented. This trend was consistently observed across all selected cutting parameters.
5) The optimum cutting parameters selected by TOPSIS are UVA-NMQL cutting conditions, 130 m/min. of cutting speed, and 0.1 mm/rev of feed rate value, when cutting force, surface roughness, cutting temperature, and material removal rate are evaluated together.

In future studies, the effect of the hybrid nanofluid MQL methods on the machining performance of the Ti-6Al-7Nb biomedical titanium alloy will be examined. In addition, it is planned to conduct a sustainability assessment in terms of carbon emissions, consumed energy, and processing costs.

Acknowledgements

The authors would like to express their appreciation to Yıldız Technical University Machining Science and Sustainability (YTU MASSUS- www.massus.yildiz.edu.tr) research group, for their laboratory facility's support of this research.

Data Availability Statement

The authors confirm that the data that supports the findings of this study are available within the article. Raw data that support the finding of this study are available from the corresponding author, upon reasonable request.

Author's Contributions

Erkin Duman: Investigation, data curation, conceptualization, validation, first draft.

Yusuf Furkan Yapan: Investigation, Writing – review & editing, Conceptualization

Mehmet Alper Sofuoğlu: Writing – review & editing, Formal analysis.

Conflict of Interest

The authors declared no potential conflicts of interest with respect to the research, authorship, and/or publication of this article.

Ethics

There are no ethical issues with the publication of this manuscript.

REFERENCES

[1] Zhang, L. C., & Chen, L. Y. (2019). A review on biomedical titanium alloys: recent progress and prospect. *Advanced Engineering Materials, 21*(4), Article 1801215. [CrossRef]

[2] Baltatu, M. S., Tugui, C. A., Perju, M. C., Benchea, M., Spataru, M. C., Sandu, A. V., & Vizureanu, P. (2019). Biocompatible titanium alloys used in medical applications. *Revista de Chimie (Rev Chim), 70*(4), 1302–1306. [CrossRef]

[3] Kumar, A., & Misra, R. (2018). 3D-printed titanium alloys for orthopedic applications. In *Titanium in Medical and Dental* Applications (pp. 251-275). Elsevier. [CrossRef]

[4] Kanapaakala, G., & Subramani, V. (2023). A review on β-Ti alloys for biomedical applications: The influence of alloy composition and thermomechanical processing on mechanical properties, phase composition, and microstructure. *Proceedings of the Institution of Mechanical Engineers, Part L: Journal of Materials: Design and Applications, 237*(6), 1251–1294. [CrossRef]

[5] Asserghine, A., Filotás, D., Németh, B., Nagy, L., & Nagy, G. (2018). Potentiometric scanning electrochemical microscopy for monitoring the pH distribution during the self-healing of passive titanium dioxide layer on titanium dental root implant exposed to physiological buffered (PBS) medium. *Electrochemistry Communications, 95*, 1–4. [CrossRef]

[6] Sarraf, M., Rezvani Ghomi, E., Alipour, S., Ramakrishna, S., & Sukiman, L. N. (2021). A state-of-the-art review of the fabrication and characteristics of titanium and its alloys for biomedical applications. *Bio-Design and Manufacturing*, 1–25. [CrossRef]

[7] Hanawa, T. (2019). Overview of metals and applications. In *Metals for Biomedical* Devices (pp. 3-29). Elsevier. [CrossRef]

[8] Ashida, M., Chen, P., Doi, H., Tsutsumi, Y., Hanawa, T., & Horita, Z. (2014). Microstructures and mechanical properties of Ti-6Al-7Nb processed by high-pressure torsion. *Procedia Engineering, 81*, 1523–1528. [CrossRef]

[9] Rotaru, H., Armencea, G., Spîrchez, D., Berce, C., Marcu, T., Leordean, D., Kim, S. G., Lee, S.-W., Dinu, C., & Băciuţ, G. (2013). In vivo behavior of surface modified Ti6Al7Nb alloys used in selective laser melting for custom-made implants: A preliminary study. *Romanian Journal of Morphology and Embryology (Rom J Morphol Embryol), 54*(3 Suppl), 791–796. [CrossRef]

[10] Shapira, L., Klinger, A., Tadir, A., Wilensky, A., & Halabi, A. (2009). Effect of a niobium-containing titanium alloy on osteoblast behavior in culture. *Clinical Oral Implants Research, 20*(6), 578–582. [CrossRef]

[11] Boehlert, C., Cowen, C., Jaeger, C., Niinomi, M., & Akahori, T. (2005). Tensile and fatigue evaluation of Ti–15Al–33Nb (at.%) and Ti–21Al–29Nb (at.%) alloys for biomedical applications. *Materials Science and Engineering: C, 25*(3), 263–275. [CrossRef]

[12] López, M. F., Gutiérrez, A., & Jiménez, J. A. (2002). In vitro corrosion behaviour of titanium alloys without vanadium. *Electrochimica Acta, 47*(9), 1359–1364. [CrossRef]

[13] Sun, Y., Huang, B., Puleo, D., Schoop, J., & Jawahir, I. S. (2016). Improved surface integrity from cryogenic machining of Ti-6Al-7Nb alloy for biomedical applications. *Procedia CIRP, 45*, 63–66.

[14] Kobayashi, E., Wang, T., Doi, H., Yoneyama, T., & Hamanaka, H. (1998). Mechanical properties and corrosion resistance of Ti–6Al–7Nb alloy dental castings. *Journal of Materials Science: Materials in Medicine, 9*, 567–574.

[15] Challa, V., Mali, S., & Misra, R. (2013). Reduced toxicity and superior cellular response of preosteoblasts to Ti-6Al-7Nb alloy and comparison with Ti-6Al-4V. *Journal of Biomedical Materials Research Part A, 101*(7), 2083–2089. [CrossRef]

[16] Singh, V., Kumar, K., & Katyal, P. (2021). Experimental investigation on surface integrity and wear behavior of Ti-6Al-7Nb alloy under rough and trim cut modes of wire electrical discharge machining. *Journal of Materials Engineering and Performance, 30*(1), 66–76. [CrossRef]

[17] Carvalho, S., Horovistiz, A., & Davim, J. (2023). Morphological characterization of chip segmentation in Ti-6Al-7Nb machining: A novel method based on digital image processing. *Measurement, 206*, Article 112330. [CrossRef]

[18] Mello, A. O., Pereira, R. B. D., Lauro, C. H., Brandão, L. C., & Davim, J. P. (2021). Comparison between the machinability of different titanium alloys (Ti–6Al–4V and Ti–6Al–7Nb) employing the multi-objective optimization. *Journal of the Brazilian Society of Mechanical Sciences and Engineering, 43*(11), 1–14. [CrossRef]

[19] del Risco-Alfonso, R., Siller, H. R., Pérez-Rodríguez, R., & Molina, A. (2019). Study of a novel ceramic tool performance in the machining of Ti-6Al-7Nb alloys. *MRS Advances, 4*(55-56), 3007–3015. [CrossRef]

[20] Gupta, A., Kumar, R., Kumar, H., & Garg, H. (2019). Optimization of process parameters during machining of Ti6Al7Nb by grey relational analysis based on Taguchi. In Journal of Physics: *Conference Series* (Vol. 2019, No. 012121). IOP Publishing. [CrossRef]

[21] Lauro, C. H., Ribeiro Filho, S. L., Brandão, L. C., & Davim, J. P. (2016). Analysis of behaviour biocompatible titanium alloy (Ti-6Al-7Nb) in the micro-cutting. *Measurement, 93*, 529–540. [CrossRef]

[22] Sharma, V. S., Singh, G., & Sørby, K. (2015). A review on minimum quantity lubrication for machining processes. *Materials and Manufacturing Processes, 30*(8), 935–953. [CrossRef]

[23] Gupta, M. K., Khan, A. M., Song, Q., Liu, Z., Khalid, Q. S., Jamil, M., Kuntoğlu, M., Usca, Ü. A., Sarıkaya, M., & Pimenov, D. Y. (2021). A review on conventional and advanced minimum quantity lubrication approaches on performance measures of grinding process. *The International Journal of Advanced Manufacturing Technology, 117*, 729–750. [CrossRef]

[24] Jagatheesan, K., Babu, K., & Madhesh, D. (2021). Experimental investigation of machining parameter in MQL turning operation using AISI 4320 alloy steel. *Materials Today: Proceedings, 46*, 4331–4335. [CrossRef]

[25] Kannan, C., Chaitanya, C. V., Padala, D., Reddy, L., Ramanujam, R., & Balan, A. (2020). Machinability studies on aluminium matrix nanocomposite under the influence of MQL. *Materials Today: Proceedings, 22*, 1507–1516. [CrossRef]

[26] Gong, L., Bertolini, R., Ghiotti, A., He, N., & Bruschi, S. (2020). Sustainable turning of Inconel 718 nickel alloy using MQL strategy based on graphene nanofluids. *The International Journal of Advanced Manufacturing Technology, 108*, 3159–3174. [CrossRef]

[27] Mosleh, M., Shirvani, K. A., Smith, S. T., Belk, J. H., & Lipczynski, G. (2019). A study of minimum quantity lubrication (MQL) by nanofluids in orbital drilling and tribological testing. *Journal of Manufacturing and Materials Processing, 3*(1), 5. [CrossRef]

[28] Roy, S., Kumar, R., Sahoo, A. K., & Das, R. K. (2019). A brief review on effects of conventional and nanoparticle-based machining fluid on machining performance of minimum quantity lubrication machining. *Materials Today: Proceedings, 18*, 5421–5431. [CrossRef]

[29] Tuan, N. M., Duc, T. M., Long, T. T., Hoang, V. L., & Ngoc, T. B. (2022). Investigation of machining performance of MQL and MQCL hard turning using nano cutting fluids. *Fluids, 7*(5), 143. [CrossRef]

[30] Makhesana, M. A., Patel, K. M., Krolczyk, G. M., Danish, M., Singla, A. K., & Khanna, N. (2023). Influence of MoS2 and graphite-reinforced nanofluid-MQL on surface roughness, tool wear, cutting temperature, and microhardness in machining of Inconel 625. *CIRP Journal of Manufacturing Science and Technology, 41*, 225–238. [CrossRef]

[31] Seyedzavvar, M., Abbasi, H., Kiyasatfar, M., & Ilkhchi, R. N. (2020). Investigation on tribological performance of CuO vegetable-oil based nanofluids for grinding operations. *Advances in Manufacturing, 8*, 344–360. [CrossRef]

[32] Sinha, M. K., Kishore, K., & Sharma, P. (2023). Surface integrity evaluation in ecological nanofluids assisted grinding of Inconel 718 superalloy. *Proceedings of the Institution of Mechanical Engineers, Part E: Journal of Process Mechanical Engineering*, Article 09544089231171042. [CrossRef]

[33] Jagatheesan, K., Babu, K., & Madhesh, D. (2023). Optimization of process parameters in turning operation using CNT based minimum quantity lubrication (MQL). *Materials Today: Proceedings, 72*, 2552–2556. [CrossRef]

[34] Ge, X., Chai, Z., Shi, Q., Liu, Y., & Wang, W. (2023). Graphene superlubricity: A review. *Friction, 2023*, 1–21. [CrossRef]

[35] Kim, K.-S., Lee, H.-J., Lee, C., Lee, S.-K., Jang, H., Ahn, J.-H., Kim, J.-H., & Lee, H.-J. (2011). Chemical vapor deposition-grown graphene: the thinnest solid lubricant. *ACS Nano, 5*(6), 5107–5114. [CrossRef]

[36] Gürgen, S., & Sofuoğlu, M. A. (2021). Advancements in conventional machining: a case of vibration and heat-assisted machining of aerospace alloys. In *Advanced Machining and Finishing* (pp. 143-175). Elsevier. [CrossRef]

[37] Koshimizu, S. (2009). Ultrasonic vibration-assisted cutting of titanium alloy. *Key Engineering Materials, 389*, 277–282. [CrossRef]

[38] Kandi, R., Sahoo, S. K., & Sahoo, A. K. (2020). Ultrasonic vibration-assisted turning of Titanium alloy Ti–6Al–4V: numerical and experimental investigations. *Journal of the Brazilian Society of Mechanical Sciences and Engineering, 42*(8), 1–17. [CrossRef]

[39] Airao, J., Nirala, C. K., & Khanna, N. (2022). Novel use of ultrasonic-assisted turning in conjunction with cryogenic and lubrication techniques to analyze the machinability of Inconel 718. *Journal of Manufacturing Processes, 81*, 962–975. [CrossRef]

[40] Shaw, M. C., & Cookson, J. (2005). *Metal cutting principles (Vol. 2)*. Oxford University Press.

[41] Molaie, M., Akbari, J., & Movahhedy, M. (2016). Ultrasonic assisted grinding process with minimum quantity lubrication using oil-based nanofluids. *Journal of Cleaner Production, 129*, 212–222. [CrossRef]

[42] Jia, D., Li, C., Zhang, Y., Yang, M., Zhang, X., Li, R., & Ji, H. (2019). Experimental evaluation of surface topographies of NMQL grinding ZrO2 ceramics combining multiangle ultrasonic vibration. *The International Journal of Advanced Manufacturing Technology, 100*, 457–473. [CrossRef]

[43] Ni, C., Zhu, L., & Yang, Z. (2019). Comparative investigation of tool wear mechanism and corresponding machined surface characterization in feed-direction ultrasonic vibration assisted milling of Ti–6Al–4V from a dynamic view. *Wear, 436*, Article 203006. [CrossRef]

[44] Veiga, C., Davim, J., & Loureiro, A. (2012). Properties and applications of titanium alloys: a brief review. *Revista Avanzada en Ciencias de Materiales, 32*(2), 133–148.

[45] Pimenov, D. Y., Mia, M., Gupta, M. K., Machado, A. R., Tomaz, Í. V., Sarikaya, M., Wojciechowski, S., Mikolajczyk, T., & Kapłonek, W. (2021). Improvement of machinability of Ti and its alloys using cooling-lubrication techniques: A review and future prospect. *Journal of Materials Research and Technology, 11*, 719–753. [CrossRef]

[46] Obikawa, T., Kamata, Y., & Shinozuka, J. (2006). High-speed grooving with applying MQL. *International Journal of Machine Tools and Manufacture, 46*(14), 1854–1861. [CrossRef]

[47] Li, K.-M., & Liang, S. Y. (2007). Performance profiling of minimum quantity lubrication in machining. *The International Journal of Advanced Manufacturing Technology, 35*, 226–233. [CrossRef]

[48] Kurgin, S., Dasch, J. M., Simon, D. L., Barber, G. C., & Zou, Q. (2012). Evaluation of the convective heat transfer coefficient for minimum quantity lubrication (MQL). Industrial Lubrication and Tribology, 64(6), 376–386. [CrossRef]

[49] Bowers, K. T., Keller, J. C., Randolph, B. A., Wick, D. G., & Michaels, C. M. (1992). Optimization of surface micromorphology for enhanced osteoblast responses in vitro. *International Journal of Oral & Maxillofacial Implants, 7*(3).

[50] Deligianni, D. D., Katsala, N., Ladas, S., Sotiropoulou, D., Amedee, J., & Missirlis, Y. (2001). Effect of surface roughness of the titanium alloy Ti–6Al–4V on human bone marrow cell response and on protein adsorption. *Biomaterials, 22*(11), 1241–1251. [CrossRef]

[51] Podany, J., Stary, V., & Tomicek, J. (2021). 3D surface roughness characteristics for biological applications. *Manufacturing Technology, 21*(6), 836–841. [CrossRef]

[52] Guilherme, A. S., Henriques, G. E. P., Zavanelli, R. A., & Mesquita, M. F. (2005). Surface roughness and fatigue performance of commercially pure titanium and Ti-6Al-4V alloy after different polishing protocols. *The Journal of Prosthetic Dentistry, 93*(4), 378–385. [CrossRef]

[53] Etri, H. E., Singla, A. K., Özdemir, M. T., Korkmaz, M. E., Demirsöz, R., Gupta, M. K., Krolczyk, J., & Ross, N. S. (2023). Wear performance of Ti-6Al-4 V titanium alloy through nano-doped lubricants. *Archives of Civil and Mechanical Engineering, 23*(3), 147. [CrossRef]

[54] Hamdi, A., Yapan, Y. F., Uysal, A., & Abderazek, H. (2023). Multi-objective analysis and optimization of energy aspects during dry and MQL turning of unreinforced polypropylene (PP): an approach based on ANOVA, ANN, MOWCA, and MOALO. *International Journal of Advanced Manufacturing Technology*, 1–18. [CrossRef]

[55] Do, D., & Nguyen, N. (2022). Applying Cocoso, Mabac, Mairca, Eamr, Topsis and Weight Determination Methods for Multi-Criteria Decision Making in Hole Turning Process. *Strojnícky časopis - Journal of Mechanical Engineering, 72*(2), 15–40. [CrossRef]

[56] Saatçi, E., Yapan, Y. F., Uslu Uysal, M., & Uysal, A. (2023). Orthogonal turning of AISI 310S austenitic stainless steel under hybrid nanofluid-assisted MQL and a sustainability optimization using NSGA-II and TOPSIS. *Sustainable Materials and Technologies, 36*, Article e00628. [CrossRef]

[57] Oussama, B., Yapan, Y. F., Uysal, A., Abdelhakim, C., & Mourad, N. (2023). Assessment of turning AISI 316L stainless steel under MWCNT-reinforced nanofluid-assisted MQL and optimization of process parameters by NSGA-II and TOPSIS. *International Journal of Advanced Manufacturing Technology, 127*, 3855–3868. [CrossRef]

[58] Khanna, N., Kshitij, G., Solanki, M., Bhatt, T., Patel, O., Uysal, A., & Sarıkaya, M. (2023). In pursuit of sustainability in machining thin-walled α-titanium tubes: An industry-supported study. *Sustainable Materials and Technologies, 36*, Article e00647. [CrossRef]

[59] Jawaid, A., Che-Haron, C. H., & Abdullah, A. (1999). Tool wear characteristics in turning of titanium alloy Ti-6246. *Journal of Materials Processing Technology, 92–93*, 329–334. [CrossRef]

[60] Usluer, E., Emiroğlu, U., Yapan, Y. F., Kshitij, G., Khanna, N., Sarıkaya, M., & Uysal, A. (2023). Investigation on the effect of hybrid nanofluid in MQL condition in orthogonal turning and a sustainability assessment. *Sustainable Materials and Technologies, 36*, Article e00618. [CrossRef]

Journal of Advances in Manufacturing Engineering
Web page info: https://jame.yildiz.edu.tr
DOI: 10.14744/ytu.jame.2023.1384436

Original Article

Surface properties of micro surface patterned Cp-Ti alloy via electrical discharge machining

Alperen Kürşat BALTA[1], Mustafa ARMAĞAN[2], Yasemin YILDIRAN AVCU[1], Eray ABAKAY[3], Egemen AVCU[*1,4]

[1]Department of Mechanical Engineering, Kocaeli University, Faculty of Engineering, Kocaeli, Türkiye
[2]Department of Mechanical Engineering, İstanbul Medeniyet University, Faculty of Engineering and Natural Sciences, İstanbul, Türkiye
[3]Department of Metallurgy and Materials Engineering, Sakarya University, Faculty of Engineering, Sakarya, Türkiye
[4]Department of Machine and Metal Technologies, Ford Otosan İhsaniye Vocational School of Automotive, Kocaeli University, Kocaeli, Türkiye

ARTICLE INFO

Article history
Received: 01 November 2023
Revised: 09 December 2023
Accepted: 12 December 2023

Key words:
Electrical discharge machining, patterned surfaces, surface morphology, surface topography, titanium alloys.

ABSTRACT

The process of machining micro surface patterns on a workpiece to improve various performance aspects of engineering materials, including wear resistance, corrosion resistance, and biocompatibility, has been a hot topic of research in recent years. Due to the restricted machinability of titanium and its alloys, it is very challenging to process micro surface patterns with exact surface geometries using traditional machining methods. Consequently, non-traditional processing techniques, such as laser, electro-erosion, and chemical etching, may overcome these obstacles. In the present study, electrical discharge machining (EDM) is used to form micro surface patterns on Cp-Ti alloy samples. First, graphite electrodes with several channels were manufactured, and then square-shaped surface patterns were processed onto Cp-Ti samples using EDM. To evaluate the machining performance of the process and surface features of the obtained micro surface patterns, the surface morphology and topography of the processed samples were investigated by scanning electron microscopy (SEM) and three-dimensional (3D) optical profilometry, respectively. The average widths of the square-shaped surface patterns along the X and Y axes were 663.7±8 μm and 609.5±4 μm, respectively. For micro surface designs with square geometry, dimensional consistency was obtained with exceedingly small amounts of variation. However, a limited number of microcracks were observed due to rapid cooling during the processing of the surface patterns. The 3D surface topographies revealed that square-shaped micro surface patterns were successfully processed on the samples, indicating that micro surface patterns can be processed on Cp-Ti samples by using the proposed methodology, which has the potential for obtaining tailor-designed surface features, particularly for biomedical and tribological applications.

Cite this article as: Balta, A. K., Armağan, M., Yıldıran Avcu, Y., Abakay, E., & Avcu, E. (2023). Surface properties of micro surface patterned Cp-Ti alloy via electrical discharge machining. *J Adv Manuf Eng*, 4(2), 46–54.

***Corresponding author.**
*E-mail address: avcuegemen@gmail.com

INTRODUCTION

Titanium and its alloys are extensively used in biomedical applications owing to their exceptional mechanical properties, strong corrosion resistance, and biocompatibility [1]. The antibacterial surface qualities of the material play the most essential role in making titanium alloys more suitable for biomedical applications and enhancing their surface properties [2]. Commercially pure titanium (Cp-Ti) is widely used in medical and surgical applications, including bio-implantable bone replacements, owing to its excellent biocompatibility, corrosion resistance, and mechanical properties [3–5]. It is frequently employed in dental implants due to its desirable biological characteristics, low Young's modulus, and adequate strength [6]. Nevertheless, its wear rate and coefficient of friction (CoF) are comparatively weak, which limits its use to situations in which sliding, fretting, and rolling contact are unavoidable [5–9].

Numerous performance features of titanium and its alloys, including tribological, corrosion, and biocompatibility, are known to be closely related to their surface and subsurface properties [10]. However, in some applications (such as tribological applications), surface and subsurface properties may not provide sufficient performance and restrict the material's application range [11]. To be biocompatible, the surfaces of materials must be hydrophilic (wettable) and rough (to ensure cell adhesion) [12, 13]. Additionally, it is desirable for titanium alloys to have hydrophobic surfaces [14]. Using micro/nano surface patterning techniques, it is possible to modify biocompatibility, protein adsorption, and cell/surface interactions [15, 16]. In biological applications, patterned surfaces enhance cell adhesion and proliferation, which is crucial for tissue engineering [17]. Moreover, patterned features may enhance the corrosion resistance of titanium alloys by modifying the surface chemistry [9, 18]. As micro-bearings, well-designed surface patterns may boost the dynamic pressure between friction pairs, trap debris produced during the friction process, and store lubricant [19]. Therefore, processing patterned surfaces on titanium and its alloys is an efficient method for improving titanium's relatively weak surface characteristics and enhancing their performance in a variety of applications [19–22].

To improve the surface properties of titanium and its alloys, various mechanical, chemical, and physical techniques such as shot peening [23], ultrasonic peening [24], laser peening [25], anodization [26], grinding [27], physical vapour deposition [28], and die-sinking electrical discharge [29] are used. Surface treatment techniques for titanium and its alloys offer both benefits and drawbacks. Despite the fact that acid etching produced a surface with high cell adhesion and a rough texture, the desired dimensional stability could not be achieved. It was also noted that acid residues produce pollution, which may result in a variety of long-term issues [30]. Anodization may generate a controlled nanoporous oxide layer, although a non-homogeneous surface distribution occurs [31]. In the literature, it was discovered that laser patterning procedures were often used. Despite the fact that laser processing generates surfaces that promote cell adhesion and proliferation, it causes substantial thermal damage to the surface and subsurface as a result of its high heat penetration [32]. As the limitations of this method have been addressed using several pattern processing techniques, a new field of study has emerged. Excellent dimensional stability and surface quality may be achieved by optimization of many parameters of die-sinking electrical discharge machining (EDM) for titanium and its alloys. EDM-roughened Ti6Al4V alloy significantly improved osteoblast cell adhesion and proliferation, as shown by Harcuba et al. [33]. Prakash and Uddin [34] reported the development of a crack-free, nonporous, biomimetic layer on a Ti-35Nb-7Ta-5Zr alloy using the EDM on hydroxyapatite powder mixed with deionized water. Karmiris-Obrataski et al. [35] conducted an experimental study on the surface topography and integrity of EDM-machined Ti6Al4V ELI. Hasçalık and Çaydaş [36] studied the influence of process parameters on Ti6Al4V material using the EDM technique with various electrode materials, including graphite, electrolytic copper, and aluminum. The graphite electrode exhibited the greatest amount of material removal and the lowest wear rates.

Literature demonstrates that the surface patterning of titanium and its alloys by EDM in collaboration with the production of surface and subsurface mechanical and biological properties is limited. In this study, a new processing approach was used to create distinctive micro surface patterns on the surface of the Cp-Ti alloy using EDM. The desired surface patterns (depth, width, and roughness, etc.) were formed on the Cp-Ti alloy for this purpose. Consequently, the surface properties and topographies of the patterned surfaces were investigated comprehensively.

MATERIALS AND METHODS

Commercially pure titanium (Cp-Ti alloys) bars with a diameter of 20 mm were obtained from TIMET (Titanium & Medical & Mining Company, Kocaeli, Turkey). Afterwards, cylindrical samples (10 mm in thickness) were cut using a semi-automatic band saw. Prior to EDM, the samples were processed with 320-, 600-, and 1200-mesh grits using automated grinding equipment to provide a homogeneous and flat surface topography.

HK-75 graphite blocks (density: 1.82 g/cm^3, electrical receptivity: 16.5 m, hardness: 72 HS), which were in the ultra-thin graphite class (average grain size: 4 μm), were chosen to machine multi-channel graphite electrodes. Then, a multi-channel graphite electrode for EDM processing of Cp-Ti samples was machined using a CNC milling machine, as the schematic of the machined electrode is given in Figure 1. Cp-Ti samples were then machined using the prepared electrode in accordance with the specifications listed in Table 1, resulting in the formation of surface patterns, as Figure 2 schematically illustrates the EDM machining of Cp-Ti samples. The EDM process parameters were selected using a trial-and-error approach. The surface pattern characteristics were selected according to a literature survey of micro-surface patterning of titanium alloys [13, 16, 22, 37–40].

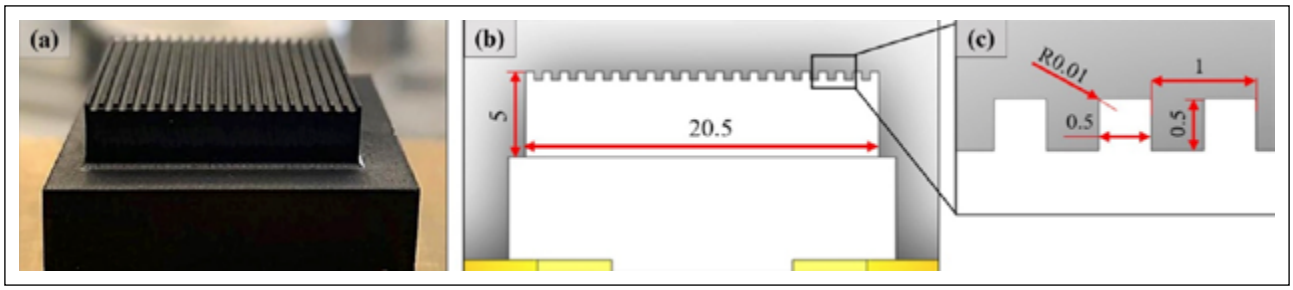

Figure 1. **(a)** Graphite electrode with multiple channels, **(b)** cross-sectional technical drawing of the surface pattern, and **(c)** dimensions of micro-patterns.

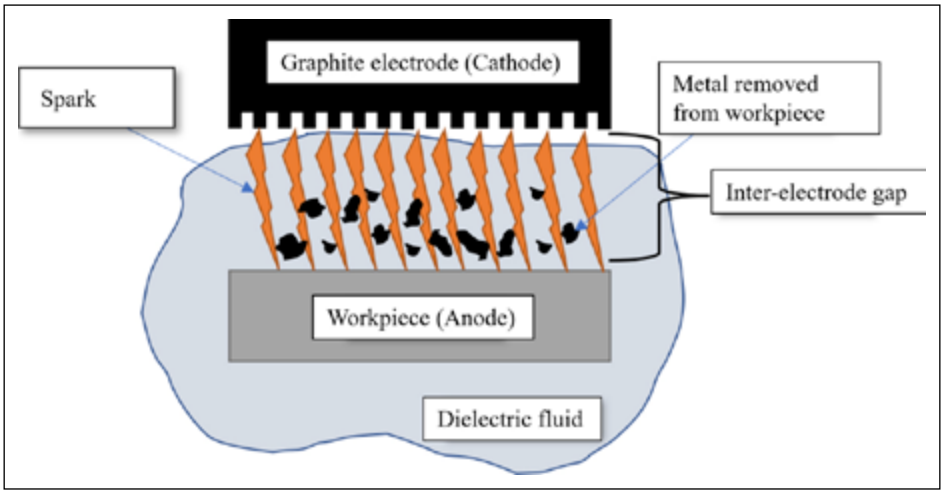

Figure 2. Schematic representation of the EDM process.

Table 1. EDM process parameters

Pulse on time	Pulse off time	Pulse current	Voltage	Servo voltage	Surface roughness
1.6 µs	6.4 µs	1A	200V	65V	0.32 Ra

EDM is a surface treatment technique that eliminates chips from the workpiece by generating high-frequency sparks between the electrode and the workpiece [40]. The target material (Cp-Ti alloy) was subjected to EDM utilizing a multi-channel electrode parallel to the X-axis of the EDM in the first stage. In the second stage, the multi-channel electrode rotated 90° and was used to machine the target material parallel to the Y axis of the EDM to obtain the square surface patterns.

The surfaces of the EDM machined samples were then cleaned for 10 minutes with alcohol and ultrasonication. A 3D optical profilometer was used to scan the surface features of the machined samples (Huvitz, Gyeonggi, Republic of Korea). The 3D surface topographies were then visualised using Mountains® 9 (Digital Surf, Besançon, France). An SEM (Jeol JSM-6060, Tokyo, Japan) with an energy dispersive spectroscopy (EDS) (Oxfords Instrument, Oxford, UK) detector was also used to analyse the surface morphologies of the samples.

The EDM machined samples were cross-sectioned using a diamond cutting disc and a precision cutter, and then the cross-sectioned specimens were moulded in resin. The moulded specimens were ground (320-, 600-, 1200-, and 2000- mesh grits) and polished (1 and 3 µm diamond suspension) using an automatic metallographic sample preparation system. In an ultrasonic bath containing alcohol, the specimens were cleaned for 10 minutes. Finally, cross-sectional examinations were performed using the SEM system previously described.

RESULTS AND DISCUSSION

The Surface Morphologies and Subsurface Features of Micro Surface Patterned Samples

In Figure 3, the surface morphologies of various channels and squares machined by EDM processing of Cp-Ti samples were given. On the X and Y axes, the average channel widths were calculated to be 362.4±4 µm and 390.8±9 µm, respectively (Fig. 3b). The channel width difference between the two axes is around 30 µm. In the X and Y directions, the average widths of the square-shaped surface patterns obtained by EDM processing of Cp-Ti alloy were 663.7±8 µm and 609.5±4 µm, respectively (Fig. 3c, d). Figure 4a shows an overall view of the surface patterns obtained via EDM. Due to electrode wear, regional melting was identified at the channel

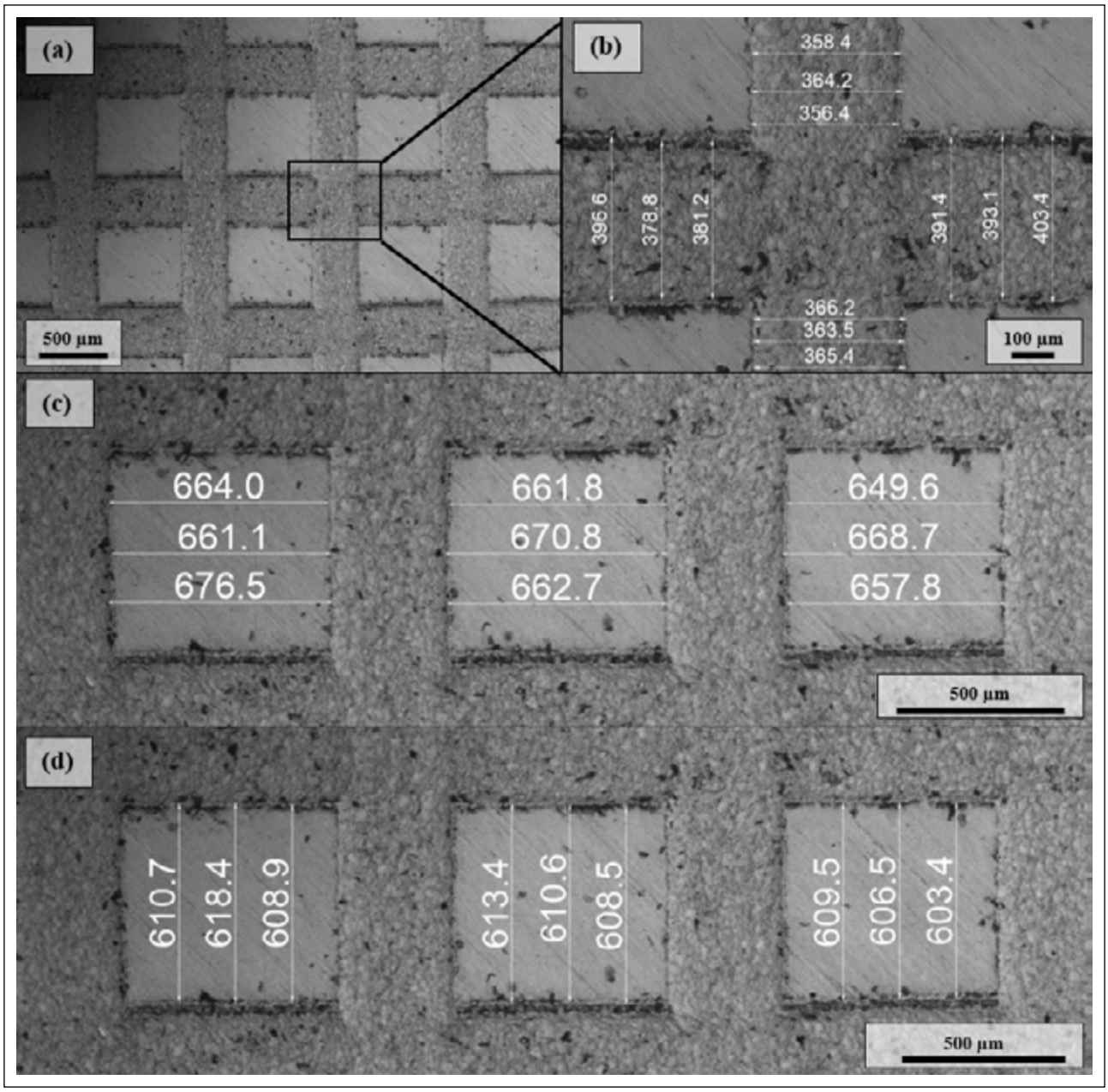

Figure 3. Micro surface pattern size measurements **(a)** General view, **(b)** Channels measurement in X and Y directions, average widths of the square-shaped surface patterns; **(c)** X direction, **(d)** Y direction.

borders along the X axis. According to the image of the channel area captured at a greater magnification (Fig. 4b), molten structures were developed because of sparks generated by electro-erosion during the EDM processing. Furthermore, a limited number of microcracks between the molten formations are also visible on the surface (Fig. 4c), which could be attributed to the rapid cooling of the machined surface features by plunge electro-erosion [41]. As a consequence of the rapid cooling of the micro pattern features, residual tensile tension is also formed. Meanwhile, dielectric liquid is used to remove debris from the surroundings that has broken off from the substance. A portion of the debris cooled on the material without removal and created the remelted layer known as the white layer [36]. Usually, surface cracks caused by the EDM process do not penetrate the substrate material. Nevertheless, cracking defects occur in the so-called white layer or re-solidified layer and in the heat-affected zone [42]. Surface defects in the form of cracking that may occur with EDM cause a decrease in the corrosion resistance of the material [43]. Tai and Lu demonstrated that EDM-machined tool steel with surface cracks would have a reduced fatigue life [44]. There is research involving the use of EDM in combination with other surface treatments to eliminate these defects and enhance the material's performance. By combining EDM, acid etching, and shot peening, Otsuka et al. [45] increased the fatigue strength and nature of cell adsorption in the Ti6Al4V alloy. Strasky et al. [46] used a combination of EDM, chemical treatment, and shot peening on the same alloy. According to reports, it improves fatigue performance and promotes osteoblast proliferation. According to these

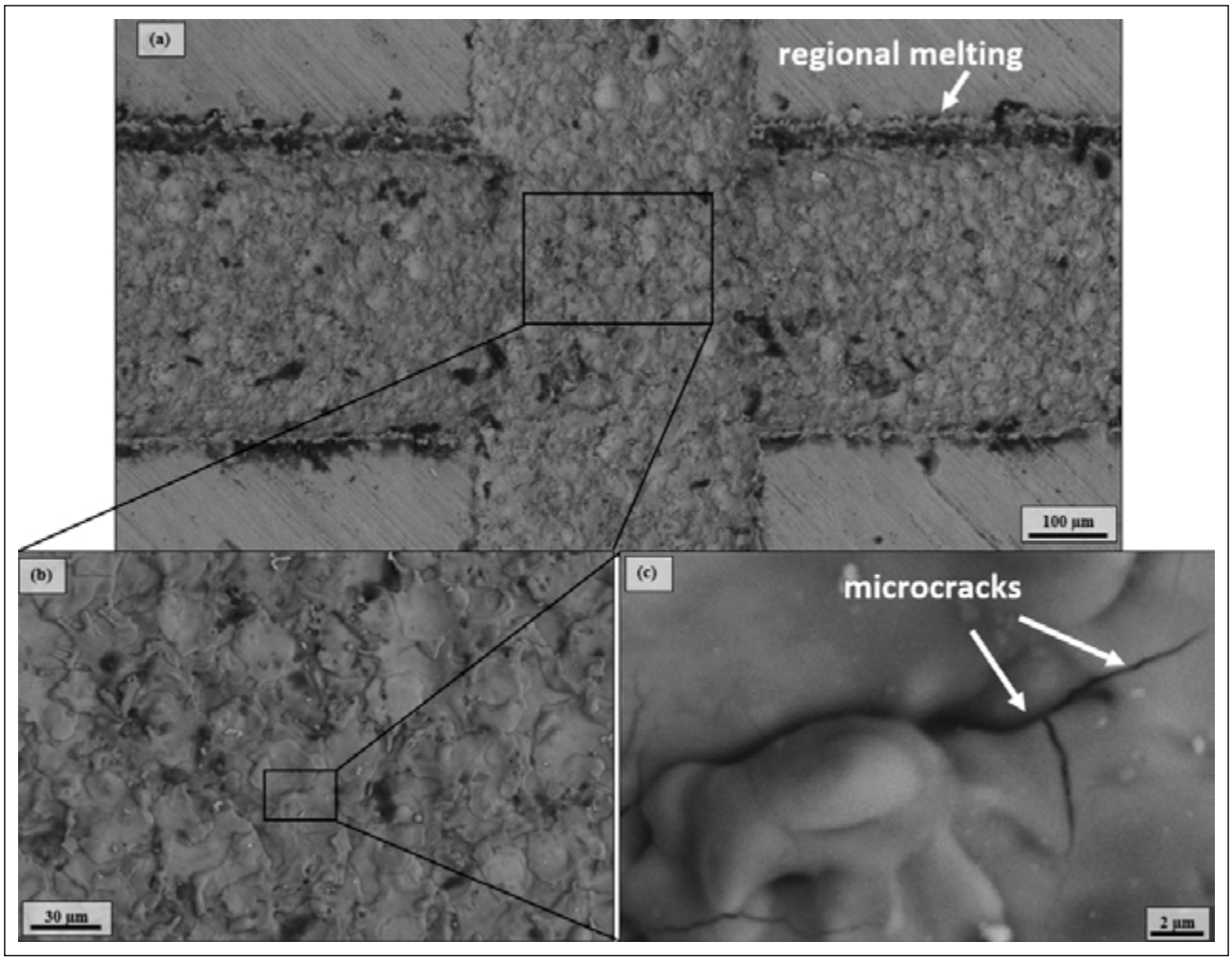

Figure 4. **(a)** Surface morphologies of the patterns, **(b)** A high magnification view of the targeted region, and **(c)** Surface microcracks.

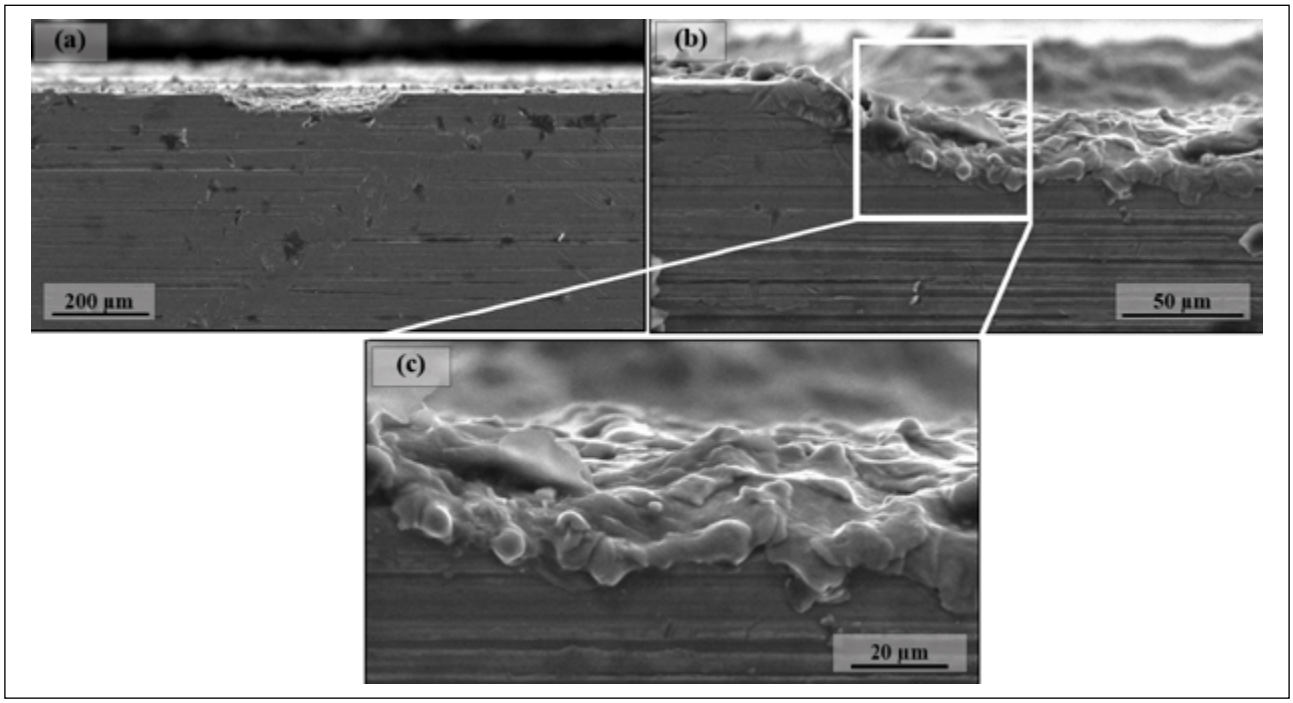

Figure 5. EDM-treated Cp-Ti alloy microstructure in cross-section **(a)** Low magnification, **(b)** High magnification, and **(c)** Overlapping recast layers.

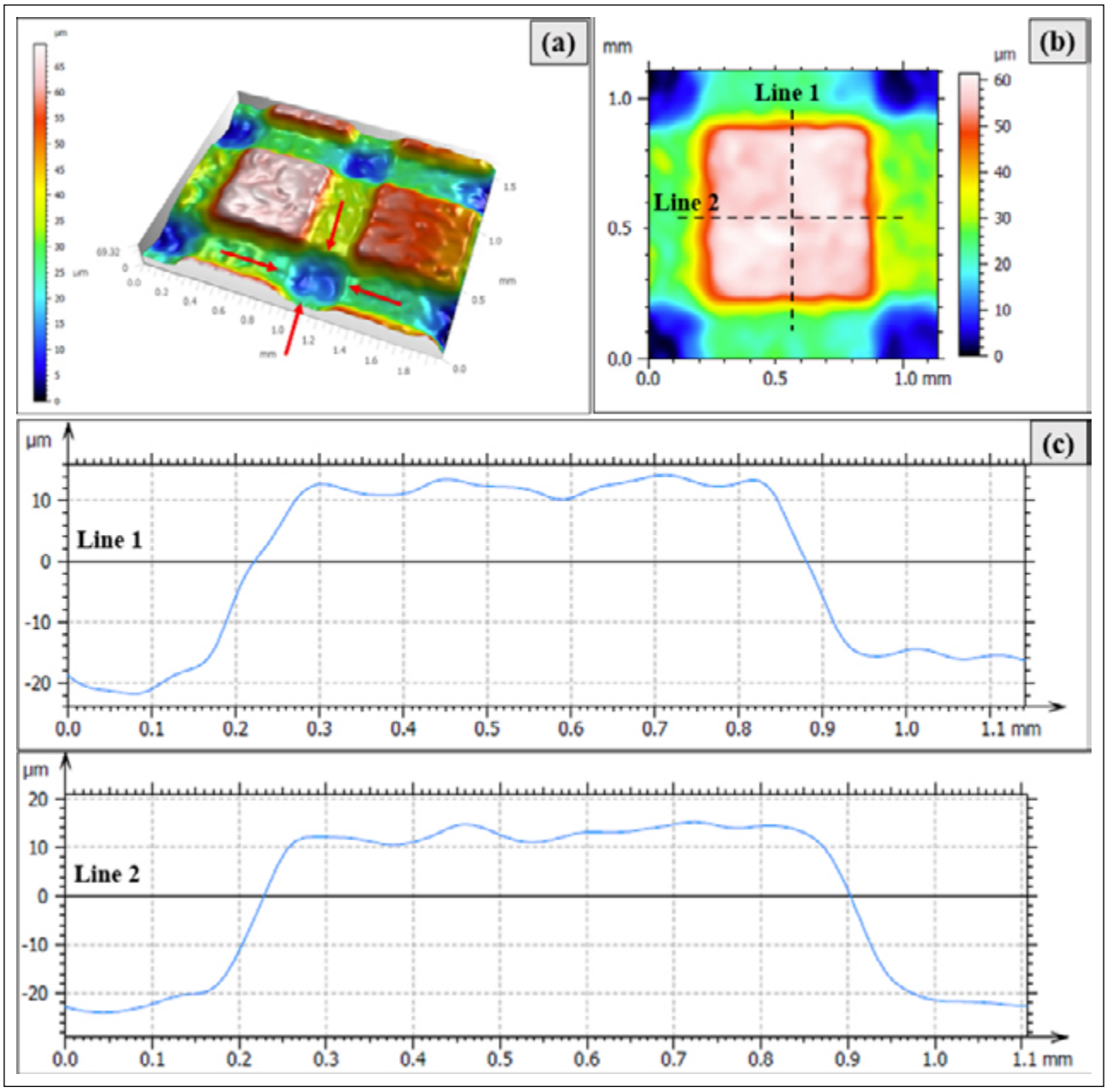

Figure 6. EDM-modified surface topographies of Cp-Ti specimens **(a)** Several square-shaped surface patterns, **(b)** A single square-shaped surface pattern, and **(c)** The surface profile of a single square-shaped surface pattern.

findings, combined machining processes may eliminate the negative effects of surface defects. However, the lack of a combined EDM process for Cp-Ti alloy in the existing literature has revealed an important topic of research.

Figure 5 shows the cross-sectional microstructure of the Cp-Ti alloy after the EDM process. It is clear that EDM causes melt pools on the near surface due to the rapid heating and cooling of the surface. Due to the current value and pulse duration, a thin molten layer was formed on the surface (Fig. 5b). The overlap of these molten layers indicates that these layers were formed between the pulse on and pulse off times. As the processing parameters (pulse on time, pulse off time, and voltage) are kept constant, the shape and geometry of the melt pools are uniform. In the sample's cross-sectional images, no cracks or crack initiation perpendicular to the surface were detected. The thickness of the remelted layer following EDM processing was approximately 40 µm, while the thickness of the untreated region was around 5 µm. The cross-sectional images provide essential information for determining the sample's heat-affected zone. This will make it easier to optimise the process parameters and achieve the desired material qualities for the desired application.

The Topographies of Surface Patterned Cp-Ti Alloy

After the EDM process, the topographies of the surface patterns were examined with an optical profilometer, and 3D surface topographies and surface profiles were analysed (Fig. 6). The melted material at the intersection of the first and second processes caused melt collapse, creating flow from the channel areas to the crater section (Fig. 6a).

A single square-shaped surface pattern topography is given in Figure 6b. It is visible that EDM processing causes relatively low surface roughness as peaks and valleys having less than 1µm height were formed on the surfaces (Fig. 6c). Examining the profiles of the square-shaped surface patterns in the x and y directions revealed that the peaks and valleys had similar features (Fig. 6c). The surface of the Cp Ti alloy was accurately patterned using multi-channel graphite electrodes, as determined by surface profile investigations.

Maressa et al.'s [47] research on laser processing of various surface patterns on Ti6Al4V alloy is used as a reference for selecting square surface patterns in the present investigation. Multiple channel surfaces, contrary micro-pits, and complicated processing forms have been shown to have a beneficial influence on bone cell behavior. Additionally, EDM machining produced channel forms with an average surface roughness of 0.1–10 µm (for Ti6Al4V alloy) [48] and 2.5–10 µm (for aluminum alloy) [49] in channel forms. In this work, a high level of surface quality was attained by reducing the Cp-Ti alloy's surface roughness in consideration of the high accuracy required for micromachining.

CONCLUSIONS

The present study comprises electrical discharge machining of micro surface patterns onto the surface of the Cp-Ti alloy. The surface morphology and topography of the processed samples were examined by scanning electron microscopy (SEM) and three-dimensional (3D) optical profilometry to assess the machining performance of the process and the surface characteristics of the produced micro surface patterns.

- The study clearly shows that micro surface patterns with excellent dimensional accuracy can be obtained following the proposed EDM methodology (i.e., designing multi-channel graphite electrodes and following the given EDM parameters). Dimensional consistency is maintained across the surface patterns in numerous square geometries.
- Due to the two-stage processing, melt collapse occurred at the intersections of the processing zones, which caused microcracks in the channel sections due to the quick cooling action. Molten spherical particles were shown by high magnification SEM photos. According to the 3D surface topographies of the processed samples, a limited surface roughness was observed on the processed features with peaks and valleys of less than 1µm in height.

The present study showed that processing micro surface patterns by using the proposed methodology has the potential to obtain tailor-designed surface features with excellent dimensional and geometrical stability and less amount of surface defects, which can pave the way for improving the biocompatibility, tribological, and corrosion performance of titanium alloys in respective scientific and industrial usage. Future studies should focus on processing and examining the subsurface properties (i.e., microstructural features and mechanical properties) of similarly processed titanium samples using electron microscopy, microhardness mapping, and indentation mapping.

Data Availability Statement

The authors confirm that the data that supports the findings of this study are available within the article. Raw data that support the finding of this study are available from the corresponding author, upon reasonable request.

Author's Contributions

Alperen Kürşat Balta: Conception, Design, Supervision, Materials, Data Collection and Processing, Analysis and Interpretation, Literature Review.

Mustafa Armağan: Conception, Design, Supervision, Materials, Data Collection and Processing, Analysis and Interpretation, Literature Review, Writer, Critical Review.

Yasemin Yıldıran Avcu: Conception, Design, Supervision, Data Collection and Processing, Writer, Critical Review.

Eray Abakay: Conception, Design, Supervision, Materials, Data Collection and Processing, Writer, Critical Review.

Egemen Avcu: Conception, Design, Supervision, Fundings, Materials, Data Collection and Processing, Analysis and Interpretation, Literature Review, Writer, Critical Review.

Conflict of Interest

The authors declared no potential conflicts of interest with respect to the research, authorship, and/or publication of this article.

Ethics

There are no ethical issues with the publication of this manuscript.

REFERENCES

[1] Alves, A. C., Oliveira, F., Wenger, F., Ponthiaux, P., Celis, J. P., & Rocha, L. A. (2013). Tribocorrosion behaviour of anodic treated titanium surfaces intended for dental implants. *Journal of Physics D: Applied Physics*, *46*(40). [CrossRef]

[2] Yuan, Z., He, Y., Lin, C., Liu, P., & Cai, K. (2021). Antibacterial surface design of biomedical titanium materials for orthopedic applications. *Journal of Materials Science & Technology*, *78*, 51–67. [CrossRef]

[3] Baldin, E. K., Santos, P. B., de Castro, V. V., Aguzzoli, C., Maurmann, N., Girón, J., ... Malfatti, C. d. F. (2021). Plasma Electrolytic Oxidation (PEO) Coated CP-Ti: Wear Performance on Reciprocating Mode and Chondrogenic–Osteogenic Differentiation. *Journal of Bio- and Tribo-Corrosion*, *8*(1). [CrossRef]

[4] Rajabi, M., Miresmaeili, R., & Aliofkhazraei, M. (2019). Hardness and wear behavior of surface mechanical attrition treated titanium. *Materials Research Express, 6*(6). [CrossRef]

[5] Avcu, Y. Y., Iakovakis, E., Guney, M., Çalım, E., Özkılınç, A., Abakay, E., ... Avcu, E. (2023). Surface and Tribological Properties of Powder Metallurgical Cp-Ti Titanium Alloy Modified by Shot Peening. *Coatings, 13*(1). [CrossRef]

[6] Aniolek, K., Barylski, A., & Kupka, M. (2021). Friction and Wear of Oxide Scale Obtained on Pure Titanium after High-Temperature Oxidation. *Materials (Basel), 14*(13). [CrossRef]

[7] Keddam, M., Makuch, N., Boumaali, B., Piasecki, A., Miklaszewski, A., & Kulka, M. (2020). Liquid Boriding of Cp-Ti and Ti6Al4V Alloy: Characterization of Boride Layers and Tribological Properties. *Surface Engineering and Applied Electrochemistry, 56*(3), 348–357. [CrossRef]

[8] Jin, J., Zhou, S., Zhao, Y., Zhang, Q., Wang, X., Li, W., ... Zhang, L.-C. (2021). Refined microstructure and enhanced wear resistance of titanium matrix composites produced by selective laser melting. *Optics & Laser Technology, 134*. [CrossRef]

[9] Avcu, E., Abakay, E., Yıldıran Avcu, Y., Çalım, E., Gökalp, İ., Iakovakis, E., ... Guney, M. (2023). Corrosion Behavior of Shot-Peened Ti6Al4V Alloy Produced via Pressure-Assisted Sintering. *Coatings, 13*(12). [CrossRef]

[10] Long, M., & Rack, H. J. (1998). Titanium alloys in total joint replacement—a materials science perspective. *Biomaterials, 19*(18), 1621–1639. [CrossRef]

[11] Vishnoi, M., Kumar, P., & Murtaza, Q. (2021). Surface texturing techniques to enhance tribological performance: A review. *Surfaces and Interfaces, 27*, Article 101463. [CrossRef]

[12] Paterlini, T. T., Nogueira, L. F. B., Tovani, C. B., Cruz, M. A. E., Derradi, R., & Ramos, A. P. (2017). The role played by modified bioinspired surfaces in interfacial properties of biomaterials. *Biophysical Reviews, 9*(5), 683–698.

[13] Priyanka, C. P., Keerthi Krishnan, K., Sudeep, U., & Ramachandran, K. K. (2023). Osteogenic and antibacterial properties of TiN-Ag coated Ti-6Al-4V bioimplants with polished and laser textured surface topography. *Surface and Coatings Technology, 474*. [CrossRef]

[14] Huang, M.-S., Wu, C.-Y., Ou, K.-L., Huang, B.-H., Chang, T.-H., Endo, K., . . . Liu, C.-M. (2020). Preparation of a Biofunctionalized Surface on Titanium for Biomedical Applications: Surface Properties, Wettability Variations, and Biocompatibility Characteristics. *Applied Sciences, 10*(4). [CrossRef]

[15] Shivakoti, I., Kibria, G., Cep, R., Pradhan, B. B., & Sharma, A. (2021). Laser Surface Texturing for Biomedical Applications: A Review. *Coatings, 11*(2). [CrossRef]

[16] Zhao, W., Zhang, J., Yu, Z., & Hu, J. (2023). Effects of bioinspired leaf vein structure on biological properties of UV laser patterned titanium alloy. Surfaces and Interfaces, 38. Article 102785. [CrossRef]

[17] Kim, H. S., Kumbar, S. G., & Nukavarapu, S. P. (2021). Biomaterial-directed cell behavior for tissue engineering. *Current Opinion in Biomedical Engineering, 17*, Article 100260. [CrossRef]

[18] Zhao, D., Han, C., Li, Y., Li, J., Zhou, K., Wei, Q., . . . Shi, Y. (2019). Improvement on mechanical properties and corrosion resistance of titanium-tantalum alloys in-situ fabricated via selective laser melting. *Journal of Alloys and Compounds, 804*, 288–298. [CrossRef]

[19] Wang, C., Huang, H., Wu, H., Hong, J., Zhang, L., & Yan, J. (2023). Ultra-low wear of titanium alloy surface under lubricated conditions achieved by laser texturing and simultaneous nitriding. *Surface and Coatings Technology, 474*. [CrossRef]

[20] Wu, Z., Xing, Y., Huang, P., & Liu, L. (2017). Tribological properties of dimple-textured titanium alloys under dry sliding contact. *Surface and Coatings Technology, 309*, 21–28. [CrossRef]

[21] Peng, Z., Zhang, X., Liu, L., Xu, G., Wang, G., & Zhao, M. (2023). Effect of high-speed ultrasonic vibration cutting on the microstructure, surface integrity, and wear behavior of titanium alloy. *Journal of Materials Research and Technology, 24*, 3870–3888. [CrossRef]

[22] Niu, Y., Pang, X., Song, C., Shangguan, B., Zhang, Y., & Wang, S. (2023). Tailoring tribological properties of Ti-Zr alloys via process design of laser surface texturing and thermal oxidation. *Surfaces and Interfaces, 37*. [CrossRef]

[23] Avcu, Y. Y., Gönül, B., Yetik, O., Sönmez, F., Cengiz, A., Guney, M., & Avcu, E. (2021). Modification of Surface and Subsurface Properties of AA1050 Alloy by Shot Peening. *Materials, 14*(21). [CrossRef]

[24] Kleiman, J., Kudryavtsev, Y., & Luhovskyi, O. (2017). Effectiveness of ultrasonic peening in fatigue improvement of welded elements and structures. *Mechanics and Advanced Technologies, 3*. [CrossRef]

[25] Mao, B., Siddaiah, A., Liao, Y., & Menezes, P. (2020). Laser surface texturing and related techniques for enhancing tribological performance of engineering materials: A review. *Journal of Manufacturing Processes, 53*, 153–173. [CrossRef]

[26] Yao, C., & Webster, T. (2006). Anodization: A Promising Nano-modification technique of titanium implants for orthopedic applications. *Journal of Nanoscience and Nanotechnology, 6*, 2682–2692. [CrossRef]

[27] Kumar, A. (2013). Optimization of Process Parameters in Surface Grinding Using Response Surface Methodology. *International Journal of Research in Mechanical Engineering & Technology, 3*, 245–252.

[28] Hacking, S., Zuraw, M., Harvey, E., Tanzer, M., Krygier, J. J., & Bobyn, J. (2007). A physical vapor deposition method for controlled evaluation of biological response to biomaterial chemistry and topography. *Journal of Biomedical Materials Research Part A, 82*, 179–187. [CrossRef]

[29] Mughal, M. P., Farooq, M. U., Mumtaz, J., Mia, M., Shareef, M., Javed, M., ... Pruncu, C. I. (2021). Surface modification for osseointegration of Ti6Al4V ELI using powder mixed sinking EDM. *Journal of the Mechanical Behavior of Biomedical Materials, 113*, Article 104145. [CrossRef]

[30] Kim, M.-H., Park, K., Choi, K.-H., Kim, S.-H., Kim, S. E., Jeong, C.-M., & Huh, J.-B. (2015). Cell Adhesion and in Vivo Osseointegration of Sandblasted/Acid Etched/Anodized Dental Implants. *International Journal of Molecular Sciences, 16*(5), 10324–10336. [CrossRef]

[31] Park, Y. J., Ha, J., Ali, G., Kim, H., Addad, Y., & Cho, S. O. (2015). Controlled Fabrication of Nanoporous Oxide Layers on Zircaloy by Anodization. *Nanoscale Research Letters, 377*, Article 10. [CrossRef]

[32] Kensy, J., Dobrzyński, M., Wiench, R., Grzech-Leśniak, K., & Matys, J. (2021). Fibroblasts adhesion to laser-modified titanium surfaces-a systematic review. *Materials (Basel), 14*(23). [CrossRef]

[33] Harcuba, P., Bačáková, L., Stráský, J., Bačáková, M., Novotná, K., & Janeček, M. (2012). Surface treatment by electric discharge machining of Ti–6Al–4V alloy for potential application in orthopaedics. *Journal of the Mechanical Behavior of Biomedical Materials, 7*, 96–105.

[34] Prakash, C., & Uddin, M. S. (2017). Surface modification of β-phase Ti implant by hydroaxyapatite mixed electric discharge machining to enhance the corrosion resistance and *in-vitro* bioactivity. *Surface and Coatings Technology, 326*, 134–145. [CrossRef]

[35] Karmiris-Obratański, P., Zagórski, K., Cieślik, J., Papazoglou, E. L., & Markopoulos, A. (2020). Surface Topography of Ti 6Al 4V ELI after High Power EDM. *Procedia Manufacturing, 47*, 788–794. [CrossRef]

[36] Hasçalık, A., & Çaydaş, U. (2007). Electrical discharge machining of titanium alloy (Ti–6Al–4V). *Applied Surface Science, 253*(22), 9007–9016. [CrossRef]

[37] Wang, Y., Hu, J., Zhang, X., Chu, Z., Ren, B., Yue, C., . . . Xian Li, L. (2023). Influence of femtosecond lase pulse sequence on the morphology and roughness of titanium surface micro-patterns. *Journal of Manufacturing Processes, 97*. [CrossRef]

[38] Etinosa, P. O., & Soboyejo, W. O. (2023). Cell/Surface Interactions and the Integrity of Ti-6AI-4V Structures: Effects of Surface Texture and RGD Coatings. *In Comprehensive Structural Integrity* (pp. 35–54). [CrossRef]

[39] Liu, C., Xin, Z., Tong, Z., Ye, Y., Ren, Y., Yu, Z., & Ren, X. (2023). Microstructure, mechanical properties and wear behaviors of TiN/Ti composite coating on laser surface textured Ti6Al4V alloy fabricated by MHz picosecond laser surface alloying. *Materials Today Communications*. [CrossRef]

[40] Tiwari, T., Dvivedi, A., & Kumar, P. (2023). Analysis of tribological behavior of dual-textured Ti-6Al-4 V alloy surfaces fabricated using a tool-mimic approach. *Tribology International, 185*.

[41] Shanbhog, N., Arunachalam, N., & Bakshi, S. R. (2022). Surface integrity studies on ZrB2 and graphene reinforced ZrB2 ceramic matrix composite in EDM process. *CIRP Journal of Manufacturing Science and Technology, 38*, 401–413. [CrossRef]

[42] Lee, H. T., & Tai, T. Y. (2003). Relationship between EDM parameters and surface crack formation. *Journal of Materials Processing Technology, 142*(3), 676–683. [CrossRef]

[43] Ntasi, A., Mueller, W.-D., Eliades, G., & Zinelis, S. (2010). The effect of Electro Discharge Machining (EDM) on the corrosion resistance of dental alloys. *Dental materials: official publication of the Academy of Dental Materials, 26*, e237–245. [CrossRef]

[44] Tai, T. Y., & Lu, S. J. (2009). Improving the fatigue life of electro-discharge-machined SDK11 tool steel via the suppression of surface cracks. *International Journal of Fatigue, 31*(3), 433–438. [CrossRef]

[45] Otsuka, F., Kataoka, Y., & Miyazaki, T. (2012). Enhanced osteoblast response to electrical discharge machining surface. *Dental Materials Journal, 31*(2), 309–315. [CrossRef]

[46] Stráský, J., Havlíková, J., Bačáková, L., Harcuba, P., Mhaede, M., & Janeček, M. (2013). Characterization of electric discharge machining, subsequent etching and shot-peening as a surface treatment for orthopedic implants. *Applied Surface Science, 281*, 73–78. [CrossRef]

[47] Maressa, P., Anodio, L., Bernasconi, A., Demir, A. G., & Previtali, B. (2015). Effect of Surface Texture on the Adhesion Performance of Laser Treated Ti6Al4V Alloy. *The Journal of Adhesion, 91*(7), 518–537. [CrossRef]

[48] Klocke, F., Schwade, M., Welling, D., & Kopp, A. (2013). Multi-scale directed surface topography machined by electro discharge machining in combination with plasma electrolytic conversion for improved osseointegration. *International Journal of Mechatronics and Manufacturing Systems, 6*, 254–269. [CrossRef]

[49] Moon, I. Y., Lee, H. W., Kim, S.-J., Oh, Y.-S., Jung, J., & Kang, S.-H. (2021). Analysis of the Region of Interest According to CNN Structure in Hierarchical Pattern Surface Inspection Using CAM. *Materials, 14*(9). [CrossRef]